Journal of Photochemistry and Photobiology A: Chemistry 207 (2009) 66–72

Contents lists available at ScienceDirect

Journal of Photochemistry and Photobiology A: Chemistry

journal homepage: www.elsevier.com/locate/jphotochem

Degradation of X-3B dye by immobilized TiO_2 photocatalysis coupling anodic oxidation on BDD electrode

Chunyong Zhang[a,b], Linjuan Gu[a,b], Yihua Lin[a,b], Yongxiang Wang[a,b], Degang Fu[a,b], Zhongze Gu[a,b,*]

[a] State Key Laboratory of Bioelectronics, Southeast University, Nanjing, 210096, China
[b] Suzhou Key Laboratory of Environment and Biosafety, Research Institute of Suzhou of Southeast University, Dushuhu Lake Higher Education Town, Suzhou, 215123, China

ARTICLE INFO

Article history:
Available online 5 February 2009

Keywords:
Reactive brilliant red X-3B dye
TiO_2 photocatalysis
Boron-doped diamond (BDD)
Advanced oxidation processes (AOPs)

ABSTRACT

Photocatalysis on nano-sized TiO_2 and electrocatalysis on boron-doped diamond (BDD) electrode, all belonged to advanced oxidation processes (AOPs) in the field of wastewater treatment, were united into one batch reactor in our experiments. Reactive brilliant red X-3B dye was used as model compound to study the combinatory effect between photocatalysis and electrocatalysis. The titania sol, deposited on glass substrate, prepared by chemical sol–gel process, was found to have anatase crystalline structure, uniform nanoparticle distribution and spherical particle morphology. The oxidants produced on BDD anodes such as hydrogen peroxide, ozone and peroxodisulfate could raise the quantum efficiency of photocatalytic processes. Initially, the performances of the separate processes in the elimination of X-3B were compared. An interesting synergistic effect was observed in the combined reactor. In order to find out the optimum conditions in color and total organic carbon (TOC) removal, the effects of the operating variables were investigated. The experimental results revealed the suitability of the combination of these two options for accelerating the removal of dye pollutants from the solution. Additionally, the assumptive reaction mechanism and the reaction kinetics were also proposed.

1. Introduction

Dye wastewater caused mainly by dyestuff and textile industry can make severe ecological problems, due to the presence of large quantities of reactive dyes which have become the focus of environmental remediation efforts [1]. Reactive brilliant red X-3B (shown in Fig. 1) is a typical reactive azo dye which has been widely used in printing industry, so it will make more sense to choose X-3B as a model compound for the present study. The remediation of wastewater containing these pollutants can be carried out by different methods, including adsorption, coagulation, chlorination, ozonation, biological treatment and permanganate, which are useful for the destruction of dissolved dyes but all have drawbacks in certain aspects [2–5]. Alternatively, advanced oxidation processes (AOPs), as a promising technique for water purification, which are based on the generated hydroxyl radicals (•OH) that able to oxidize a broad range of organic contaminants non-selectively in a short period of time (with rate constants on the order of 10^6–10^9 mol L^{-1} s^{-1}), have attracted much attention in recent years. Interestingly, AOPs also offer different routes to •OH production, allowing easier tailoring of the process for specific treatment requirements.

The heterogeneous photocatalytic oxidation process using nano-sized semiconductor as catalyst under UV light irradiation is one of the most effective options among the existing AOPs [6]. Titanium dioxide, the best one exhibiting many unique properties among a series of semiconductors, has been extensively studied in the degradations of various pollutants, especially in dye wastewaters [7–9]. The focus of many investigators is to apply oxidants such as ozone, hydrogen peroxide into photocatalytic system, thereby improving the performance significantly and to gain a synergistic effect [10]. Another report showed that a series of peroxides such as peroxodisulfate and percarbonate ions could also raise the efficacy of photocatalytic process [11].

Boron-doped diamond (BDD) is also a versatile material which has been applied in many occasions, such as electrochemical analysis, electro-synthesis, etc. It exhibits unique properties such as wide potential window, low background currents, excellent chemical stability, and high overpotential for water electrolysis. As anode, it allows the production of a mixture of strong oxidants like hydroxyl radicals, hydrogen peroxide and ozone easily used in the AOPs under several mechanisms [12]. Also, the sulfate ions in the solution can be oxidized to peroxodisulfate easily on BDD electrode [13]. Recently, many investigators have reported the successful applications of BDD in the degradation or removal of phenols, dyes, herbicides and other toxic chemical treatment [14–16]. In this

* Corresponding author at: State Key Laboratory of Bioelectronics, Southeast University, Nanjing, 210096, China. Tel.: +86 2583795635; fax: +86 2583795635.
E-mail addresses: batzcy3000@yahoo.cn (C. Zhang), roujing202@126.com (L. Gu), editorlin@126.com (Y. Lin), wyx1982@seu.edu.cn (Y. Wang), fudegang@seu.edu.cn (D. Fu), gu@seu.edu.cn (Z. Gu).

1010-6030/$ – see front matter © 2009 Elsevier B.V. All rights reserved.
doi:10.1016/j.jphotochem.2009.01.014

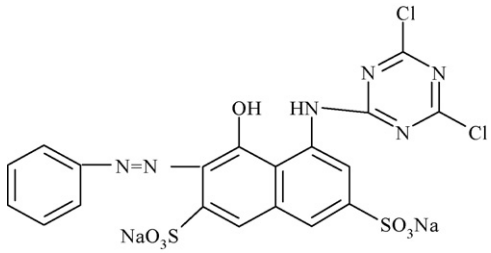

Fig. 1. Molecular structure of X-3B dye (chemical formula = $C_{19}H_{10}O_7N_6Cl_2S_2Na_2$).

paper, we united BDD electrocatalysis and TiO_2 photocatalysis into one reactor to improve the performance, for both options involved •OH as main oxidizing species, their combination would surely raise the yield of •OH. Interestingly, the mixture of oxidants produced on BDD electrode just meet the need of photocatalytic process. In fact, much efforts have been made to develop systems combining two different AOPs [17,18]. But the practice differs from the so-called photoelectrochemical oxidation [19], which is based on the driving force by UV light on light-sensitive electrode such as Ti substrate coated with TiO_2/RuO_2, resulting in higher quantum yields for the inhibition to the electron/hole pairs recombination. There was one report concerning the united use of electrolysis and photocatalysis but the reaction was taken place in two separated unit reactors [20]. To the best of our knowledge, we found few reports had appeared on the combined use of these two options.

Therefore, the goal of this work was to investigate the combinatory effect between TiO_2 photocatalysis and BDD electrocatalysis. In particular, the influencing factors such as supporting electrolyte, pH, applied current density and initial dye concentrations on the removal of X-3B dye were studied, the possible reaction mechanism and the reaction kinetics were also proposed.

2. Experimental

2.1. Materials

Reactive brilliant red X-3B dye, $Ti(OBu)_4$, NaCl, Na_2SO_4, NaOH, KNO_3, Na_3PO_4, Na_2CO_3 and H_2SO_4, all purchased from Shanghai Chemical Reagent Co. (Shanghai, China), were of analytical grade and used without further purification. Deionized water was obtained using AVP-2-35G-01 Water-system (Millipore, USA). A 9-W U-shaped UV lamp with maximal emission at 365 nm was purchased from Yaming (Shanghai, China).

BDD electrode (boron-doped diamond thin film deposited on p-Si(1 1 1) substrate by CVD technology) was supplied by Kanagawa Academy of Science of Technology(Japan), the same size stainless steel plate with high dimensional precision and fine-polished surface was supplied by Nanjing Yanziji Manufacturing Factory (Nanjing, China), both electrodes were square type plate with the effective surface area of 3.24 cm^2.

2.2. Preparation and immobilization of titania hydrosol

TiO_2 sol was prepared with $Ti(OBu)_4$ as precursor following the procedures described elsewhere [21]. TiO_2 sol was obtained with uniform stable and semi-transparent characteristics. The sol can maintain homogenous distribution for quite a long-time without sedimentation of delamination phenomena.

The sol was deposited on glass substrate by means of spin-coating. First, the sol rinsed the inner surface of glass cell, the sol thin film was then under heat treatment at 70 °C for 1 h, and the procedure was repeated for 8 times. The titania sol was loaded on the inner surface of the glass reactor with excellent strength.

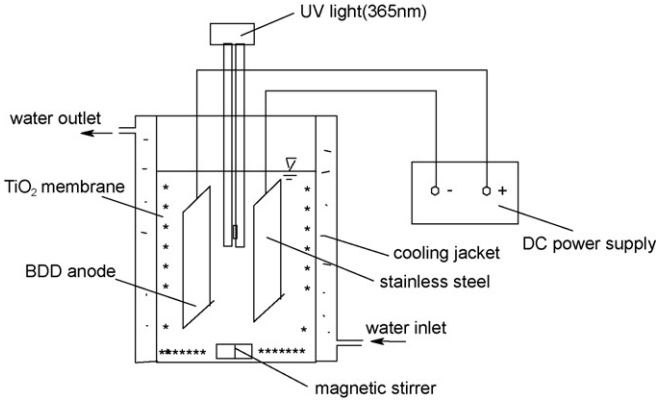

Fig. 2. Schematic of the coupled reactor used for contaminants degradation.

2.3. Analytical apparatus

HITACHI UV-Vis-NIR spectrophotometer (U-4100, Japan) was used to determine the concentration of X-3B, the determination wavelength was 512 nm which is the maximum absorption wavelength of X-3B. The determined absorbance was converted to concentration through the standard curve of X-3B. Excellent linear fit between concentration of X-3B and corresponding UV absorbance was shown in the scope of 0–100 mg/l ($R = 0.9999$). The total organic carbon (TOC) was determined using 1020A TOC analyzer (O.I.Analytical, USA), and the pH value of reaction medium was controlled by an acidimeter (pH S-2, Shanghai REX Instrument Factory, China). The color destruction efficiency was calculated by $\eta\,(\%) = (c_0 - c)/c_0 \times 100 = (A_0 - A)/A_0 \times 100$, where c_0 and c were the concentration of X-3B when reaction time was 0 and t, respectively, while A_0 and A were the corresponding absorbance of X-3B before and after the degradation.

2.4. Degradation experiments

Experiments were mainly performed in a laboratory scale electro/photo chemical reactor consisted of 50 ml cylindrical one-compartment glass cell, the inner surface of the glass cell was coated with titania sol (Fig. 2). The BDD plate served as anode, while the same size stainless steel plate as cathode, the electrode gap was set as 10 mm. The reactor also fitted with a UV lamp which was located in the cylindrical center. Water samples with desired initial concentration of X-3B and salt concentrations were oxidized under galvanostatic mode in the presence of UV light irradiation, the processed volume was 25 ml in each run. The reaction temperature was

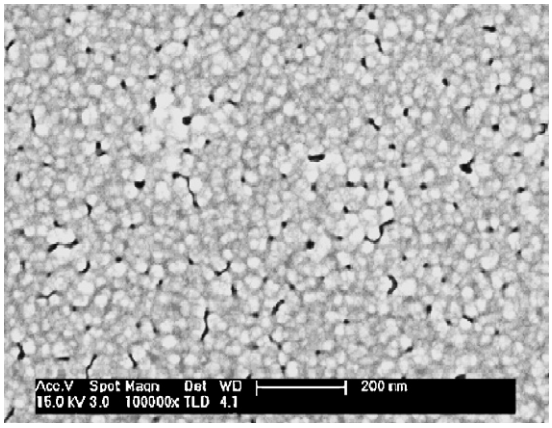

Fig. 3. SEM image of the titania.

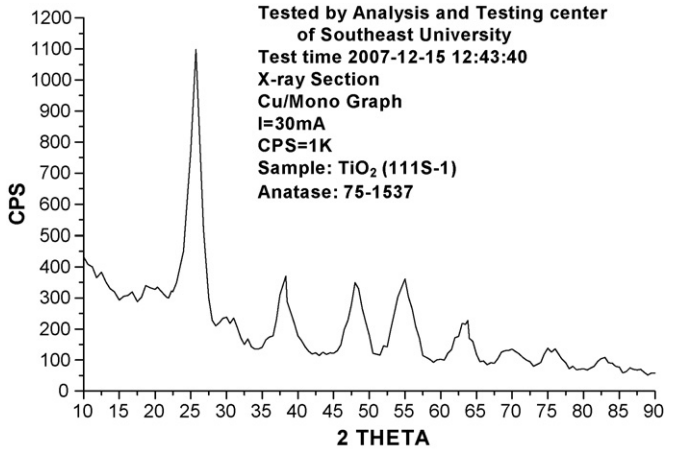

Fig. 4. XRD analysis of the titania prepared (*X* coordinate: diffraction angle 2θ; *Y* coordinate: relative intensity (a.u.)).

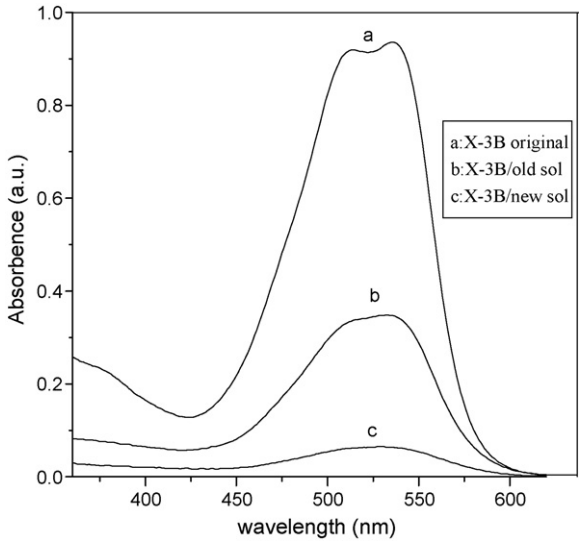

Fig. 5. Adsorption curve of X-3B on titania sol.

maintained at 25 °C by a cooling jacket and the reaction solution was continuously stirred at a constant stirring rate of 350 rpm in order to keep homogeneous. The pH value was adjusted with 1.0 M H_2SO_4 or 1.0 M NaOH to the desired values. Before each reaction, the surface of electrode should be washed clean by ethanol and ultrapure water. The reactions were started by turning on UV light and DC power supply and quenched immediately with power switch at predefined times. The treated water samples were collected at 5 min, 10 min, 20 min and 30 min, and the concentrations of residual X-3B in the reaction mixture were analyzed by the UV–vis and TOC method described above.

3. Results and discussion

3.1. SEM and XRD analysis of titania hydrosol

The sol particle morphology, particle size and composition were investigated by SEM and XRD, and the samples were fabricated on silica glass by means of spin-coating.

SEM micrograph shows that well-developed TiO_2 sol particles disperse in colloidal system (Fig. 3). The sol particles obviously have good particles distribution in aqueous medium. Also, the sol particles indicate that it retards the aggregation and growth of well-dispersed sol particles, resulting in smaller grain size of TiO_2 sol particles with the mean size of about 30 nm.

The XRD pattern of TiO_2 sol sample shows the presence of peaks (2θ = 25.4°, 38.0°, 48.0°, 54.7° and 63.1°), which is regarded as an attributive indicator of anatase phase TiO_2 crystallites (Fig. 4). The characteristic phase state of sol can be considered as anatase crystalline structure due to the appearance of standard diffraction peaks with somewhat weak scattering peaks characterization [22]. The sol particles have very broad diffraction peaks at (1 0 1) plane (2θ = 25.4°), whose nature is due to their very small grain size. The sol samples do not appear any other diffraction peaks of new crystal phase besides anatase structure. Since this kind of material exhibits excellent photocatalytic activity [23], it is chosen in our study.

3.2. Adsorption study

The heterogeneous photocatalysis is mainly occurred in catalyst/solution interfacial layers, so the adsorption and affinity properties between reactants and photocatalyst surface play important roles on determining overall reaction rate [24,25]. As have been extensively studied, titania materials of various kinds all exhibit adsorption properties for organic molecules [26]. While BDD electrode had an inert surface of weak adsorption capabilities for both •OH and reactants [12], only the case of TiO_2 was considered.

The effect of adsorption–desorption equilibrium was investigated between 50 mg/l X-3B and immobilized photocatalysts in aqueous medium. 25 ml X-3B solution was taken into the reactor and was stirred and bubbled with air for at least 2 h in darkness at 25 °C to allow equilibration of the system so that the loss of compound due to adsorption could be taken into account. An as-prepared titania film and a film used for several times were utilized for comparative study, the residual X-3B concentrations in bulk solution were measured by UV–vis spectrophotometer.

Fig. 5 shows that the absorption intensity of X-3B at 512 nm in bulk solution both decreases in comparison with original X-3B solution. The decrease of X-3B concentration due to adsorption by photocatalyst is 46.7 mg/l and 31.8 mg/l for as-prepared and "old" TiO_2 film, respectively. Regarding this strong adsorption capability, the two key factors are ascribed to the positive charge characteristic of TiO_2 nanoparticles surface since anionic dye X-3B molecule loads negative charge [22], another one is attributed to the well-dispersed sol nanoparticles, respectively.

3.3. Comparison of different reaction systems

In order to clarify the feasibility of the combination of photocatalysis with electrocatalysis, different reaction systems of the same size were employed to study the performance in X-3B decolorization, listed as (1) BDD alone; (2) BDD with UV light, without TiO_2; (3) TiO_2 photocatalysis with UV light; (4) BDD + UV + TiO_2; (5) BDD + UV + TiO_2 + aeration. The air rate was set to 5.0 l/h by a small magnetic air pump. The experimental conditions were set as follows: initial concentration of X-3B (c_0), 50 mg/l; current density (I_{appl}), 25.2 mA/cm^2; pH 2.72 (adjusted with 1.0 M H_2SO_4). The time for removing color completely was understudied for each reaction system, and the results were illustrated in Fig. 6.

It can be deduced that photocatalysis coupled with electrocatalysis in one reactor will degrade pollutants faster than individual option. The results obtained show some interesting phenomena. The UV light can accelerate the degradation rate of dye pollutants in BDD electrocatalysis, which is not a new finding. Comninellis [27] proposed a mechanism for the oxidation of organics with concomitant oxygen evolution, which assumed that both organic oxidation and oxygen evolution take place on BDD via intermediation of •OH,

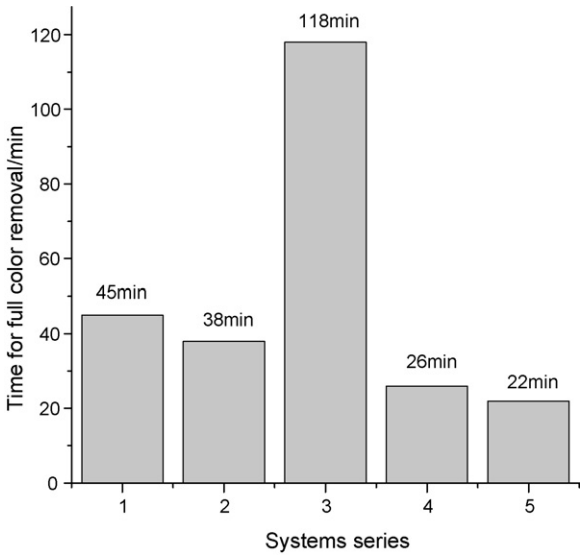

Fig. 6. Comparison on degradation performance of different reaction systems.

generated from the discharge of water (reactions (1) and (2))

$$BDD + H_2O = BDD(^{\bullet}OH) + H^+ + e^- \quad (1)$$

$$BDD(^{\bullet}OH) = BDD + (1/2)O_2 + H^+ + e^- \quad (2)$$

$$BDD(^{\bullet}OH) = BDD + (1/2)H_2O_2 \quad (3)$$

$$BDD(^{\bullet}OH) + SO_4^{2-} = BDD + (1/2)S_2O_8^{2-} + OH^- \quad (4)$$

Then, part of the •OH are combined to form hydrogen peroxide in reaction (3), while sulfate ions can be oxidized to form peroxodisulfate according to reaction (4). These reagents are all electron acceptors which are known to be very powerful oxidants and can act as a mediator for organics oxidation at higher temperature or with UV light irradiation [12] (reactions (5)–(8)). The UV light fitted in the reactor surely play important roles in activating these peroxides, resulting in a rise in oxidation efficiency. Considering the contribution of individual UV photolysis, an additional experiment was performed. It was found that the UV light showed rather weak ability in degrading X-3B directly in the absence of TiO_2 (3.1% within 60 min), so the effect could be omitted in most cases.

$$H_2O_2 = 2^{\bullet}OH \quad (5)$$

$$H_2O_2 + e_{CB}^- = {}^{\bullet}OH + OH^- \quad (6)$$

$$S_2O_8^{2-} + e_{CB}^- = {}^{\bullet}SO_4^- + SO_4^{2-} \quad (7)$$

$$^{\bullet}SO_4^- + H_2O = SO_4^{2-} + {}^{\bullet}OH + H^+ \quad (8)$$

The photocatalytic process needs nearly 2 h to remove color completely, indicating the limited oxidizing capability of the immobilized catalytic system. The reactive species involved may all do contributions to some extent in the degradation process (reactions (9)–(12))

$$TiO_2 + UV = h^+ + e_{CB}^- \quad (9)$$

$$h^+ + H_2O = {}^{\bullet}OH + H^+ \quad (10)$$

$$e_{CB}^- + O_2 = {}^{\bullet}O_2^- \quad (11)$$

$$^{\bullet}O_2^- + H^+ = {}^{\bullet}HO_2 \quad (12)$$

It is an exciting result that an enhanced effect appears in the combined reactor. Full color removal achieved within 26 min indicates a combined effect of two options, the synergism between photocatalysis and electrocatalysis seems exist. Both BDD electrode and TiO_2 film produces •OH on their surfaces, and a portion of them may react directly with X-3B. As have been well established by the literature, oxidation of pollutants at BDD anode occur under mass transfer control mainly in a thin liquid film near to the electrode surface, where the concentration of •OH is very high. Similar phenomenon also exists in photocatalytic systems. But the adding salts (SO_4^{2-}) can trap part of these •OH to form peroxides and diffuse into the whole solution to allow full contact with X-3B. Then •OH are set "free" by activating these mixture of oxidants (H_2O_2, $S_2O_8^{2-}$) with UV light, thus promotes the performance as well as the generation of more •OH on the surfaces of both BDD electrode and TiO_2 film. In another hand, in the photocatalytic processes implicating TiO_2 particulates, one practical problem is the undesired electron/hole recombination for lack of proper electron acceptor or donor, and the mixture of oxidants produced on BDD electrode may just meet this need. The combinatory effect is rather interesting and further discussions are put forward in later sections.

Last, the time decreases from 26 min to 22 min with aeration, possibly as a result that the oxygen in air added into the solution and the vigorous stirring effect of bubbles promote the performance. The results may be attributed to two factors: (1) the strengthened diffusion of the reactants and intermediates towards the surfaces of both TiO_2 membrane and BDD electrode leads to the higher reaction rate and current efficiency and (2) more efficient generation of •OH by TiO_2.

3.4. Effect of operating variables for color removal

In order to clarify the degradation behavior in the combined reactor, different operating parameters were applied in the following study. Two options involved behaved quite differently in the combined system, so the compromise study between them appeared to be very necessary.

3.4.1. Effect of supporting electrolyte

Due to the mass transfer limitations of direct oxidation processes in electrochemical cells, a trial often practiced is to introduce in electrolyte an oxidizable species (like sulfate) during electrolysis. The peroxide formation avoids the side reaction of oxygen evolution and can act as a mediator during oxidation [13]. A series of supporting electrolytes with the concentration of 50 mM were introduced into the reactor. The experiments were performed under conditions of initial concentration of X-3B (c_0), 50 mg/l; current density (I_{appl}), 25.2 mA/cm^2 and no pH adjustment.

It can be seen from Fig. 7 that electrolytes play important roles during reaction, different electrolytes presented in the solution induce rather different degradation behaviors of X-3B. In the combined reactor, the effects of both options should be taken into account simultaneously. Chantal et al. [28] made studies on the influence of inorganic salts on the photodegradation of dyes, and the inhibition of photocatalytic properties in presence of ions was often explained by the scavenging of •OH by ions. At neutral pH, the inhibition sequence of inorganic salts followed the decreasing order: carbonate > phosphate > sulfate > chloride > nitrate. But in our case, the properties of salts are also vital for the performance of anodic oxidation on BDD electrode. For example, in the case of sodium chloride as supporting electrolyte, most •OH generated on BDD anode may be consumed to produce active chlorine according to reactions (13) and (14) instead of being reacted directly with organic pollutants.

$$BDD(^{\bullet}OH) + Cl^- = BDD + (1/2)Cl_2 + OH^- \quad (13)$$

$$Cl_2 + H_2O = Cl^- + HClO + H^+ \quad (14)$$

Active Cl_2 or HClO are strong oxidants that have been observed being able to degrade organic pollutants effectively [29], and they can also attack the azonic group of X-3B. In the point of photocatal-

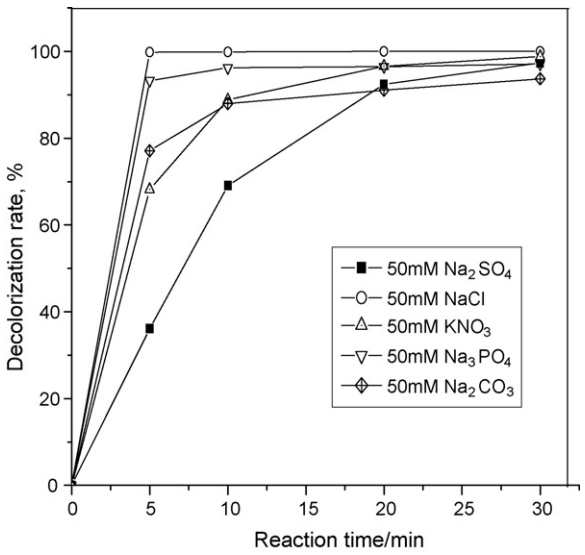

Fig. 7. Decolorization rate of X-3B versus different supporting electrolytes (c_0: 50 mg/l, I_{appl}: 25.2 mA/cm^2).

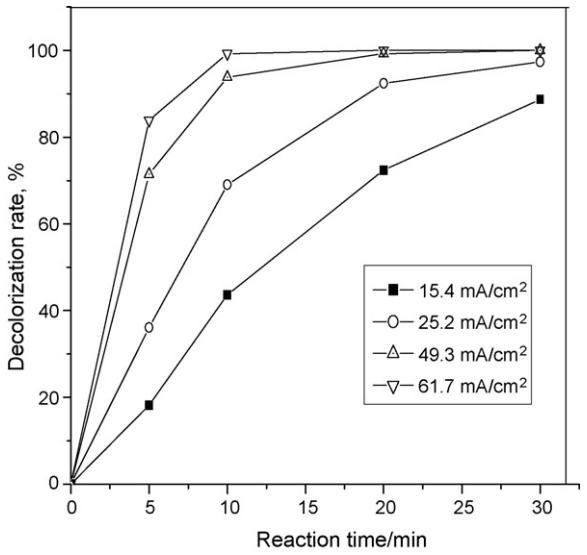

Fig. 9. Color removal rate of X-3B versus applied current density (c_0: 50 mg/l, 50 mM Na_2SO_4).

ysis, the formation of a double layer of salts on the surface of TiO_2 decreases the adsorption of dyes. In another hand, these anions can all be oxidized into corresponding peroxides on BDD surface, which together with the original salts may also pose a complex influence on the performance of titania, a more detailed description of this phenomenon is still under study.

Usually, sulfates are the most widely studied electrolytes among the existing "oxidizable salts". The peroxodisulfate can be produced at high concentration without any problem of mass transport limitations, and it is well mixed with the wastewater for maximizing the contact of oxidants and organic species [12]. Sulfates were chosen for further study owing to these advantages.

3.4.2. Effect of pH

The dependence of degradation rate of X-3B on initial pH values was illustrated in Fig. 8, the pH value of original 50 mg/l X-3B was 5.44.

The pH effect may be the most important variable for both BDD electrocatalysis and TiO_2 photocatalysis, but it is difficult to elucidate clearly the mechanism of this effect on the coupled process. For photocatalysis, it dictates the surface charge properties of photocatalyst, size of aggregation it formed and the absorption behavior for target organic pollutants [30]. For electrocatalysis, it strongly influences the activities of the generated oxidants such as •OH, H_2O_2 and $S_2O_8^{2-}$ [31]. Acidic condition (pH 3.41) does not favor the oxidation of X-3B, but with less acidic cases color removal rate increases to a maximum at pH 6.94. As reported in [18], when the pH increased, the active hydroxyl groups on TiO_2 increased too. Consequently, a faster generation of •OH accelerated the X-3B degradation. But after 20 min, extended reaction time had "smoothing" effect on further decolorization of X-3B for all cases.

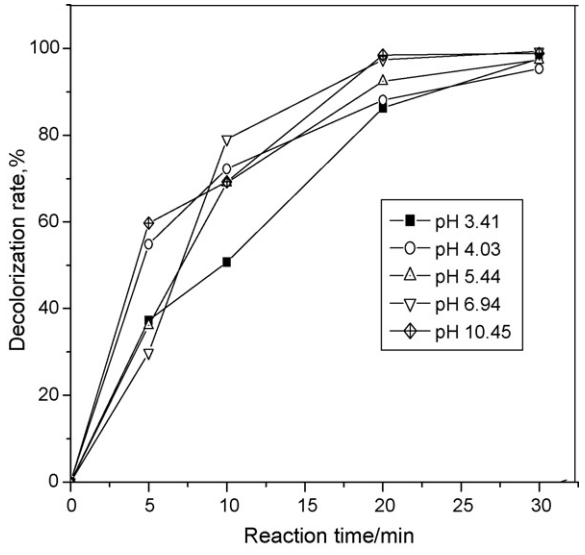

Fig. 8. Color removal rate of X-3B versus initial pH of electrolyte solutions (c_0: 50 mg/l, I_{appl}: 25.2 mA/cm^2, 50 mM Na_2SO_4, pH range from 3.41 to 10.45).

3.4.3. Effect of applied current densities

Lawton and Robertson [32] proposed that under constant I_{appl}, the electro-generation of •OH at BDD surface was uniform and it could be greatly enhanced with increasing I_{appl}, thus promoted the generation of active oxidants from electrochemical oxidation processes. Different current densities ranging from 15.4 mA/cm^2 to 61.7 mA/cm^2 were applied to study the effects involved, and the results were illustrated in Fig. 9.

There is a clear trend towards an enhancement of the oxidation power as the current densities increases, for the formation rates of active species are certainly higher at higher I_{appl} [33]. As expected, increasing I_{appl} resulted in a faster decolorization of X-3B, due to a great charge entering the cell. As I_{appl} increases from 15.4 mA/cm^2 to 49.3 mA/cm^2, the degradation rate is increased almost proportional to I_{appl}. But the performances differ little between the cases of I_{appl} at 49.3 mA/cm^2 and 61.7 mA/cm^2. It have been reported that under constant I_{appl}, the electro-generation of •OH at BDD surface is uniform, the higher I_{appl} causes the production of larger amount of •OH favoring the removal of organics with time, but consuming greater specific charge because these oxidants are generated to a less reactive extent due to faster acceleration of their non-oxidizing reactions, which results in the heating of the solution and the decrease of current efficiency [34]. Thus, proper choice of I_{appl} opens great possibility to achieve best degradation efficiency, while prevents the electrode fouling problems frequently encountered.

3.4.4. Effect of initial X-3B concentrations

The effects of initial X-3B concentrations were depicted in Fig. 10 with varying range from 25 mg/l to 100 mg/l. The degradation rate

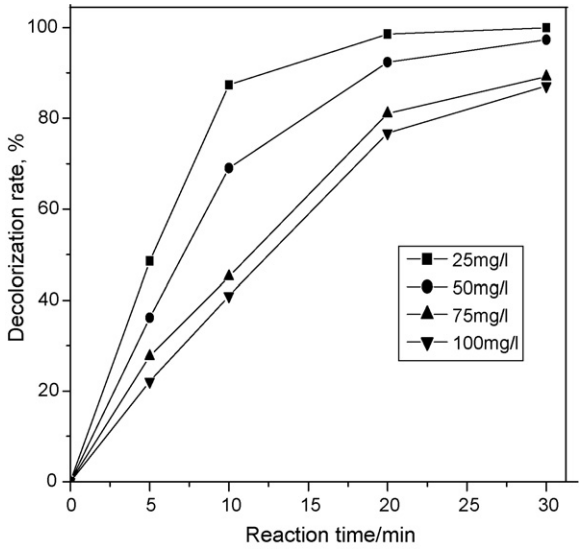

Fig. 10. Color removal rate of X-3B versus initial concentration of X-3B (I_{appl}: 25.2 mA/cm^2, 50 mM Na_2SO_4).

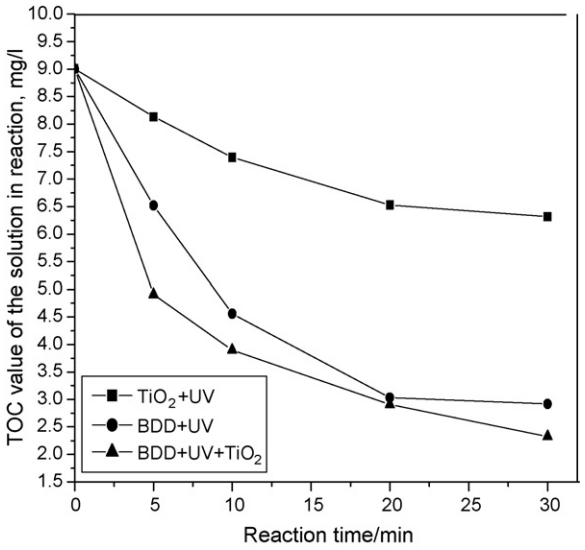

Fig. 12. TOC decay with reference to electrolysis time for the mineralization of X-3B with three different systems (c_0: 50 mg/l, I_{appl}: 25.2 mA/cm^2, pH 2.72).

decreases with increasing initial concentrations of X-3B, which is accord with the results reported in [20] and [31]. This can be explained by the relatively limited oxidation capability of the system under a certain current density value, for the main contribution of the degradation process is the formation of active oxidants. According to the trend, the more rapid destruction can be obtained in the solution with lower X-3B concentrations. Interestingly, little difference is shown when c_0 increases from 75 mg/l to 100 mg/l, which means the method is also applicable to cases with higher concentration of X-3B.

Besides, according to the practice reported in [20], we made a similar trial that the reaction was taken place in two separated reactors. The processes were tested with batch mode experiments and different initial paths were used, listed as (1) first, under electrolysis for 10 min then under photocatalysis for another 10 min (BDD 10 min + TiO_2 10 min); (2) TiO_2 10 min + BDD 10 min; (3) combination of electrolysis and photocatalysis (TiO_2 + BDD (10 + 10) min).

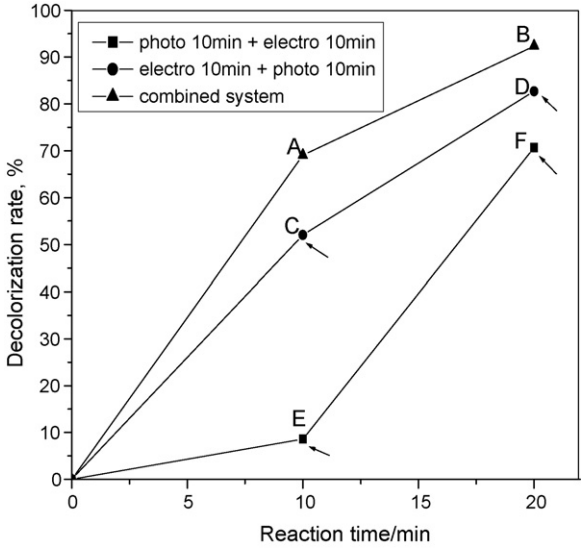

Fig. 11. Comparison on degradation performance of different reaction system combinations (c_0: 50 mg/l, I_{appl}: 25.2 mA/cm^2, 50 mM Na_2SO_4).

The results shown in Fig. 11 again confirm the superiority of the combined system over individual ones. The decolorization rate at 10 min is 8.6%, 52.1% and 69.1% for photocatalysis alone, electrolysis alone and the combined option, respectively. From point C to point D, the removal rate achieved through photocatalysis is about 30%, which is much higher than 8.6%. Also from point E to point F, the removal rate through electrolysis is about 60%, which is also higher than 52.1%. This may be attributed to two factors: (1) c_0 at point C and point E are all lower than 50 mg/l, the removal efficiency is certainly better according to the trend shown in Fig. 10; (2) a few peroxides have formed at point C, which may be very helpful to the subsequent photocatalytic process.

3.5. Mineralization and reaction kinetics study of X-3B

The mineralization trend of X-3B at the photocatalytic reactor, electrocatalytic reactor and the coupled reactor in Section 3.3 were chosen to be examined, respectively, as a function of electrolysis time, which aimed to determine whether the dye was not only decolorized but also degraded, the result was illustrated in Fig. 12.

The quantity of TOC removed at 5 min is 9.7%, 27.6%, 44.9% for systems 1, 2 and 3, respectively. Many reports [13,35,15] have suggested the action of OH or HO_2 radicals during AOPs. These loosely adsorbed (quasi free) •OH are very reactive and can lead to mineralization of organic compounds via electrochemical oxygen transfer reactions (EOTR) [36]. It is also found that electrocatalysis may do more contributions in TOC removal, which confirms the active character of BDD electrode towards the mineralization of X-3B. Faster mineralization of X-3B is achieved by the combined means, which leads to the nearly 75% destruction of molecules and formation of CO_2 as final product.

Besides, the TOC removal rate is found to be lower than color removal rate and no correlation between them is shown. This indicates that the cleavage of azonic group is the first step of the oxidation processes follows by instantaneous breakdown reactions contributing to TOC removal. It can further infer that most of the aromatic intermediate products are persistent and degrading less rapidly, and they are presumably further oxidized through ring-rupturing reactions into aliphatic compounds and the mineralization reactions to CO_2 may finally occur.

Table 1
The degradation kinetics of X-3B fitting pseudo-first order reaction.

Expt.	Reaction equations	Rate constants, k (min^{-1})	Half life, $t_{1/2}$ (min)	Correlation coefficient, R^2	r, X-3B degradation ratio (TOC)	η, X-3B degradation ratio (color)
UV + TiO_2	$\ln(c/c_0) = -(0.012 \pm 0.002)t$	0.012 ± 0.002	57.8 ± 8.3	0.9608	29.8%	45.6%
BDD + UV	$\ln(c/c_0) = -(0.130 \pm 0.008)t$	0.130 ± 0.008	5.3 ± 0.3	0.9437	67.6%	94.7%
BDD + UV + TiO_2	$\ln(c/c_0) = -(0.150 \pm 0.009)t$	0.150 ± 0.009	4.6 ± 0.2	0.9354	74.2%	100.0%

The three catalytic oxidation processes of X-3B are described with pseudo-first order kinetics model, which is $-dc/dt = kt$, where k is pseudo-first order rate constant (by a regression analysis method). It can be seen from Table 1 that X-3B decay all have deviations to certain extent in fitting pseudo-first order ($R \sim 0.95$). This is explained by the competitive consumption of •OH at the BDD surface by parallel oxidation reaction with intermediate compounds, as reported in [37]. By comparison of k and r value (X-3B degradation ratio at 30 min), it indicates that the overall degradation efficiency is enhanced to certain extent in the coupled reactor.

The synergistic effect involved in TOC removal appears to be weak, but it does exist. As a simplified mode, we use k value for calculation: $\varepsilon = (k_3 - k_2 - k_1)/k_3 = (0.150 - 0.130 - 0.012)/0.150 = 0.053$, where ε is the synergistic factor. The possible reasons are listed as follows: (1) The effects of adding sulfate into the catalytic systems are controversial, few reports [38] show weak or adverse influences. (2) The maximal emission of the UV lamp is 365 nm, which has limited activating ability towards peroxodisulfate [39], so some effects illustrated above are not so desirable as we had expected. (3) Due to the high complexity of the reactions in the combined system, there is no possibility at present to realize a precise and complex chemical analysis as an inline method and interference effects must be additional expected [40]. On the other hand, both oxidation pathway and efficiency of the process seem to depend on the nature of the pollutants. The operating conditions used in the present study need to be further optimized to achieve better synergistic effect.

Summarizing the present state of research, a more careful approach was recommended to be put forward in this field.

4. Conclusions

We set up a new combination in which TiO_2 photocatalysis and BDD electrocatalysis being united into one reactor, the feasibility of X-3B removal was studied in bulk degradation varying the electrolyte and operating conditions. As for the cases with sulfate as supporting electrolyte were mainly investigated, the degradation efficiency of color and TOC was enhanced to certain extent in the combined reactor, possibly as a result of synergistic effect in which the yield of hydroxyl radicals was raised. Similar success could be speculated in the degradation of other dyes, phenols, herbicides, halocarbon, toxins and various pollutants using this combined technology. Also the catalytic oxidation in suspension TiO_2 coupling BDD electrocatalysis might also be feasible for the removal of various contaminants.

Acknowledgments

This study is supported by United Program of Production, Research & Study of Guangdong Province, China. The study on detection and degradation of trace contaminants in environment (2007). C.Y. Zhang wishes to express thanks to Prof. *Akira Fujishima* of Kanagawa Academy of Science of Technology (Japan) for supporting us with high-quality BDD electrode. Also, we appreciate the kind offer of Prof. *Haruo Inoue* of Tokyo Metropolitan University (Japan) for presenting our work for publication in the special issue of JPP. A.

References

[1] J. Chen, M. Liu, J. Zhang, Y. Xia, L. Jin, Chemosphere 53 (2003) 1131–1136.
[2] I.A. Arslam, Balcioglu, Dyes Pigments 43 (1999) 95–108.
[3] S.H. Lin, C.F. Peng, Water Res. 28 (1994) 277–282.
[4] A.S. Koparal, Y. Yavuz, U.B. Ogutveren, Electroadsorpion of Acilan, Water Environ. Res. 6 (2002) 521–525.
[5] O. Tunay, I. Kabdasli, G. Eremektar, D. Orhon, Water Sci. Technol. 34 (1996) 9–16.
[6] F.J. Benitez, J.L. Acero, F.J. Real, J. Hazard. Mater. B 89 (2002) 51–65.
[7] X.-H. Qi, Z.-H. Wang, Y.-Y. Zhuang, Y. Yu, J.-L Li, J. Hazard. Mater. B 118 (2005) 219–225.
[8] M. Saquib, M. Abu Tariq, M. Faisal, M. Muncer, Desalination 219 (2008) 301–311.
[9] M.D. Hernandez-Alenso, M. Juan, J.M. Coronado, A. Maira, J. Appl. Catal. B: Environ. 39 (2002) 257–267.
[10] J. Fernandez, J. Kiwi, J. Baeza, J. Freer, C. Lizama, H.D. Mansilla, Appl. Catal. B: Environ. 48 (2004) 205–211.
[11] K.B. Dhanalakshmi, S. Anandan, J. Madhavan, P. Maruthamuthu, Solar Energy Mater, Solar Cell 92 (2008) 457–463.
[12] A. Fujishima, Y. Einaga, T.N. Rao, D.A. Tryk, Diamond Electrochemistry, Elesvier Bkc, Tokyo, Japan, 2005, pp. 1–573.
[13] M. Panizza, G. Cerisola, Electrochim. Acta 51 (2005) 191–199.
[14] A. Morao, A. Lopes, M.T. Pessoa de Amorim, I.C. Goncalves, Electrochim. Acta 49 (2004) 1587–1595.
[15] C. Saez, M. Panizza, M.A. Rodrigo, G. Cerisola, J. Chem. Technol. Biotechnol. 82 (2007) 575–581.
[16] B. Boye, E. Brillas, B. Marselli, P.A. Michaud, C. Comninellis, G. Farnia, G. Saudona, Electrochim. Acta 51 (2006) 2872–2880.
[17] C. Flox, P.-L. Cabot, F. Centellas, J.A. Garrido, R.M. Rodriguez, C. Arias, E. Brillas, Appl. Catal. B: Environ. 75 (2007) 17–28.
[18] T.E. Agustina, H.M. Ang, V.K. Pareek, Chem. Eng. J. 135 (2008) 151–156.
[19] R.T. Pelegrini, R.S. Freire, N. Duran, R. Bertazzoli, Environ. Sci. Technol. 35 (2001) 2849–2853.
[20] M.G. Meelavannan, M. Revathi, C. Ahmed Basha, J. Hazard. Mater. 149 (2007) 371–378.
[21] Y. Hu, C. Yuan, J. Crystal Growth 274 (2005) 563–568.
[22] Y. Xie, C. Yuan, X. Li, Colloids Surf. A 252 (2005) 87–94.
[23] Y. Kotani, T. Matode, A. Matsuda, J. Mater. Chem. 11 (2001) 2045–2048.
[24] M. Lewandowski, D.F. Ollis, Appl. Catal. B: Environ. 43 (2003) 309–327.
[25] C. Hu, Y.Z. Wang, H.X. Tang, Appl. Catal. B: Environ. 35 (2001) 95–105.
[26] C.N. Rusu, J.T. Yates, J. Phys. Chem. B 104 (2000) 12292–12298.
[27] C. Comninellis, Electrochim. Acta 39 (1994) 1857–1862.
[28] G. Chantal, L. Hinda, H. Ammar, K. Mohamed, E. Elimame, H. Jean-Marie, J. Photochem. Photobiol. A: Chem. 158 (2003) 27–36.
[29] M. Murugananthan, G. Bhaskar Raju, S. Prabhakar, J. Chem. Technol. Biotechnol. 80 (2005) 1188–1197.
[30] M. Panizza, C. Bocca, G. Cerisoda, Water Res. 34 (2000) 2601–2605.
[31] M. Murugananthan, S. Yoshihara, T. Rakuma, N. Uehara, T. Shirakashi, Electrochem. Acta 52 (2007) 3242–3249.
[32] L.A. Lawton, P.K.J. Robertson, Environ. Sci. Technol. 33 (1999) 771–775.
[33] H. Shi, J. Qu, A. Wang, J. Ge, Chemosphere 60 (2005) 326–333.
[34] P. Canizares, J. Garcia-Gomez, C. Saez, M.A. Rodrigo, J. Appl. Electrochem. 34 (2004) 87–94.
[35] A. Lair, C. Ferronato, J.-M. Chovelon, J.-M. Herrmann, J. Photochem. Photobiol. A: Chem. 193 (2008) 193–203.
[36] A. Kapalka, G. Foti, C. Comninellis, Electrochim. Acta 53 (2007) 1954–1961.
[37] F. Al Monani, Sep. Purif. Technol. 57 (2007) 85–93.
[38] Y. Wang, C.S. Hong, Water Res. 33 (1999) 2031–2036.
[39] J. Matos, J. Laine, J.M. Herrmann, Appl. Catal. B: Environ. 18 (1998) 281–291.
[40] M.E. Henry Bergmann, J. Rollin, Catal. Today 124 (2007) 198–203.